SOLIDIFICATION IN NEUTRON STAR CORES

V. Canuto* and S. M. Chitre†

Institute for Space Studies
Goddard Institute for Space Studies
National Aeronautic and Space Administration
New York, New York 10025

We report a calculation aimed at showing that a system of strongly interacting baryons under sufficiently high pressure ($P \simeq 10^{30}$ atm) and densities ($\rho > 10^{15}$ g/cc) minimizes the energy by arranging the constituents in a lattice structure rather than in a fluid phase. The required pressures and densities do indeed exist in the interior of neutron stars, and the interesting question is to find out if the matter inside a neutron star can crystallize. Previous work on the structure of neutron stars[1] indicated that the crust is composed of ordinary nuclei arranged in a crystalline structure.[2]

By increasing in density, i.e., by going towards the center of the star, the nuclei become more and more neutron-rich, and at a density of $\rho \gtrsim 1.4 \times 10^{14}$ g/cc they dissolve into a fluid. The interior of the star beyond this density is believed to be composed of superfluid matter. The aim of this paper is to report on a computation intended to give credibility to the hypothesis that the deep interior of the star is a solid crystal made of neutrons and hyperons. An earlier attempt in this direction was reported by Anderson and Palmer.[3] They used the law of corresponding states after having adjusted an average nucleon-nucleon potential to a Lennard-Jones shape, to find that a gas of neutrons solidifies at $P = 1.7 \times 10^{27}$ atm or $\rho \gtrsim 1.4 \times 10^{14}$ g/cc. Similar results were reported by Clark and Chao,[4] who improved on the original method. Since the nucleon-nucleon potential is less repulsive than the L. J. potential (remark made by H. A. Bethe), and the tail, because of dipole-dipole interaction, has a different curvature than that given by one pion exchange potential, the argument based on the law-corresponding state cannot be made with total confidence. It, however, calls for a quantum mechanical computation either to confirm or to reject the conclusion. We have used the t-matrix approach, which has been successfully employed to describe quantum crystals like solid ^{3}He.[5] We originally employed the variational method of Nasanow[6] but soon found that the treatment of angular momentum and spin-dependent correlation functions was difficult to incorporate in the formalism. We adopted the t-matrix for which the Brueckner type of analysis can be a useful guide. Up to second order, the energy per particle is known to be[7]

$$E/N = \tfrac{3}{4}\hbar\omega + \tfrac{1}{2}\sum_{ij}\int \Phi_{ij} V_{ij} \psi_{ij} dr_i dr_j \qquad (1)$$

Higher-order terms will be discussed in the final part of the paper. Each particle is thought to be localized at a lattice site of a specific crystal structure (say FCC); ω is the frequency of oscillation of the particle at the lattice site.

In Equation 1, Φ_{ij} is the two-body uncorrelated wave-function, which is the

* Also with the Department of Physics, City College of the University of New York, New York, N.Y.

† On leave of absence from Tata Institute of Fundamental Research, Bombay, India.

product of two gaussian functions centered at the lattice sites $\mathbf{R}_1$ and $\mathbf{R}_2$, respectively,[7] i.e.

$$\Phi_{ij} = \phi(i)\phi(j) = \Phi(R)\phi(r)$$

$$= \frac{\alpha^{3/2}}{(\pi/2)^{3/4}} \exp\left[-\alpha^2(\mathbf{R} - \boldsymbol{\Delta})^2\right] \cdot \frac{\alpha^{3/2}}{(2\pi)^{3/4}} \exp\left[-\frac{\alpha_2}{4}(\mathbf{r} - \boldsymbol{\delta})^2\right] \quad (2)$$

where $(\boldsymbol{\delta}, 2\boldsymbol{\Delta}) = \mathbf{R}_1 \mp \mathbf{R}_2$ and $\alpha = (m\omega/\hbar)^{1/2}$. On the other hand, $\psi(r)$ is the correlated two-body wave function that is taken to satisfy the Bethe-Goldstone equation[5, 7, 8]

$$[T(1) + T(2) + U(1) + U(2) + V_{12}]\Psi = \epsilon\Psi \quad (3)$$

where the one-body potentials U's are given by

$$\phi(i)U(i)\phi(i) = \sum_j \int \phi(i)\phi(j)V_{ij}\Psi_{ij}dr_j. \quad (4)$$

The frequency of oscillation ω is obtained by solving the set of equations 1–4 simultaneously. After separating center of mass and relative coordinates, equation 3 reduces to $(\psi_{ij} = \psi(R)\psi(r))$

$$\left[-\frac{\hbar^2}{m}\nabla_r^2 + \frac{m}{4}\omega^2(\mathbf{r} - \boldsymbol{\delta})^2 + V(r)\right]\psi(r) = (\epsilon - 3\hbar\omega)\psi(r) \quad (5)$$

The wave-function ψ has to be taken dependent upon M_s, the projection of the total spin S. This is because the energy depends upon the spin configuration used in the crystal structure under consideration. We will in fact specify the lowest energy configuration by arranging the spins in a specific order. It is obvious that a configuration with all spins parallel will, for instance, give too much energy because of the presence of $^3P_1$, which is always repulsive at any distance. The general wave-function is therefore written as (see equation of Ref. 9)

$$\psi^{SM_s}(r) = \sum_{l,J} i^l\sqrt{4\pi(2l+1)}(l0SM_s \mid JM_s)\psi_{lJ}^{M_s}(r)\mathcal{Y}_{lJ}^{M_s}(\Omega) \quad (6)$$

After considering the three possibilities (A) $S = 0$, $M_s = 0$, (B) $S = 1$, $M_s = 0$, (C) $S = 1$, $M_s = 1$, and substituting the three resulting wave-functions in equation 5, we get three sets of coupled differential equations. The coupling of various waves (within a prescribed spin configuration) is due to the term $\mathbf{r}\cdot\boldsymbol{\delta} = r\delta\cos\theta$ that couples odd and even waves. One important question relates to the number of angular momentum waves to be included in (B). We had originally worked out the problem including up to $l = 2$. Following a remark of H. Bethe, we have extended the computation up to $l = 4$ and subsequently up to $l = 6$. The $l = 4$ case gave answers lower than the $l = 2$ case, whereas we found little difference between $l = 4$ and $l = 6$. The two-body equation will be written here for the more general case, $l = 6$.

The three sets of equations for the case A, B, and C contain 7, 13, 18 coupled differential equations each, for a total of 38 partial waves ($^1S_0 \cdots {}^1I_7$; $^3S_1 \cdots {}^3I_7$;).

$S = 0$, $M_s = 0$. In this case the inclusion of $l = 6$ waves gives rise to 7 coupled equations that are written in the following compact form:

$$F_l^{J\prime\prime} + (E - U_l^J)F_l^J + (-1)^{l+1}\frac{a^4xd}{2}\left[\frac{l}{2l+1}F_{l-1}^{J-1} - \frac{l+1}{2l+1}F_{l+1}^{J+1}\right] = 0$$

($l = 0, \cdots, 6$) and $\underline{l = J}$.

$\underline{S = 1, M_s = 0}$

$$G_l^{J\prime\prime} + (E - U_l^J)G_l^J + (-1)^{l+1}\frac{a^4xd}{2}\left[\frac{l}{2l+1}\sum_{J'}(l+1\,0\,1\,0\,|\,J'0)^2G_{l+1}^{J'}\right.$$
$$\left. - \frac{l+1}{2l+1}\sum_{J''}(l-1\,0\,1\,0\,|\,J''0)^2G_{l-1}^{J''}\right] = 0$$

($l = 0, \cdots, 6$) and J takes the values compatible with $|l-1| \leqslant J \leqslant l+1$ and likewise the sum over J' and J'' follows the rule $|l| \leqslant J' \leqslant l+2$, $|l-2| \leqslant J'' \leqslant l$.

$\underline{S = 1, M_s = 1}$ **(7)**

$$H_l^{J\prime\prime} + (E - U_l^J)H_l^J + (-1)^{l+1}\frac{a^4xd}{2}\left[\frac{l}{2l+1}\sum_{J'}(l+1\,0\,1\,1\,|\,J'\,1)^2H_{l+1}^{J'}\right.$$
$$\left. - \frac{l+1}{2l+1}\sum_{J''}(l-1\,0\,1\,1\,|\,J''\,1)^2H_{l-1}^{J''}\right] = 0$$

The notation is same as above. We have used the Reid soft-core nucleon-nucleon potential for V_{ij}^s.

$$U_l^J = \frac{1}{4}a^4x^2 + \frac{mr_0^2}{\hbar^2}V_{ij}^s + \frac{l(l+1)}{x^2}$$

$$F_l^J, G_l^J, H_l^J = \psi_l^J/r, \quad E = \frac{mr_0^2}{\hbar^2}\left(\epsilon - 3\hbar\omega - \frac{1}{4}\frac{\hbar^2}{m}\alpha^4\delta^2\right), \quad a = \alpha r_0$$

$$x = r/r_0, \quad d = \delta/r_0, \quad \rho = \frac{m\gamma}{r_0^3} \; (\gamma = 4, \text{F.C.C.}; \; \gamma = 2, \text{B.C.C.})$$

Once the ψ's are known for each spin and angular momentum component, the energy can readily be computed by using equation 1. The wave-function for the $^1S_0$ state is shown in FIGURE 1, along with the t-matrix $V\psi$ for the same state. If we write $\psi = \phi(r)g(r)$, where $g(r)$ is a correlation function, we see that $g(r)$ can almost be represented by a step function $\theta(r - r^*)$ where r^* is about 0.468 for $\rho = 3 \times 10^{15}$ g/cc and k turns out to be $\lesssim 0.25$. For $r \sim 0$ the behavior of ψ is dominated entirely by $g(r)$ that has to be almost zero to make the t-matrix ($\sim\psi V$) finite near the origin; away from it, where g tends to one, the gaussian behavior dominates, as seen from the peak occurring almost at $\mathbf{r} = \boldsymbol{\delta}$, the first neighbor distance. As stated earlier, different spin arrangements in different crystal structures give different answers. We tried several configurations until we were able to minimize the energy by choosing an *F.C.C.* lattice with a spin arrangement such that any two neighboring nucleons on the same cube have opposite spin projections. The most unfavorable case was a B.C.C. lattice with one cube filled with all spins up and the second cube with all spins down. The reason for this can easily be traced back to the frequent appearance of $^3P_1$, a wave that is always repulsive for any nucleon distance.

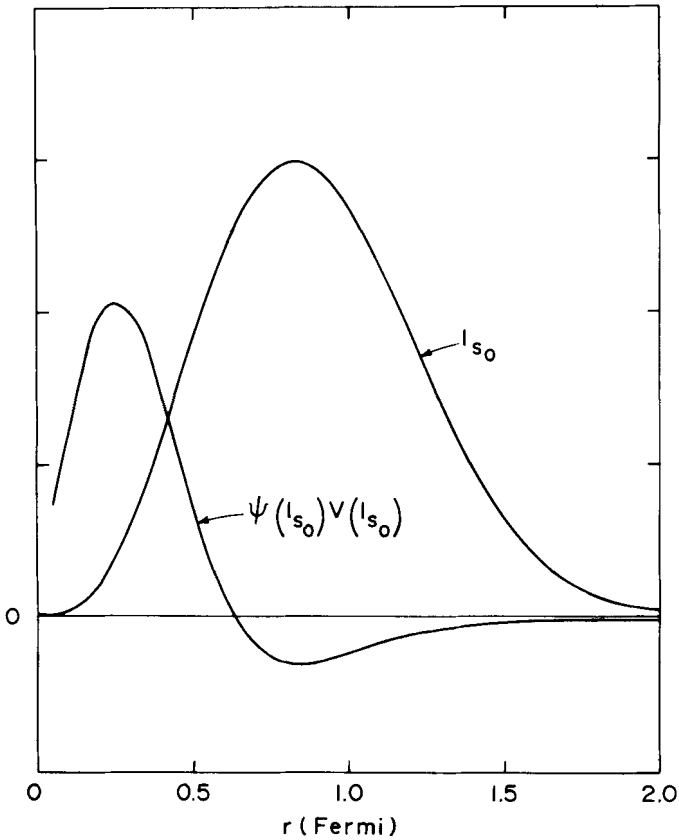

FIGURE 1. Wave function ψ for the singlet state $^1S_0$ and the product $\psi(^1S_0)\ V(^1S_0)$ at $\rho = 3.34 \times 10^{15}$ g/cm^3 for the nearest neighbor distance $\Delta = 0.891$ fermi.

We also found, as expected, that the fewer the protons, the lower the energy. The results presented in TABLE 1 refer to a system of pure neutrons. In the range $1.6 \leqslant \rho_{15} \leqslant 5.0$ the spread of the single particle wave function α^{-1} turns out to be $0.238 \leqslant \alpha^{-1} \leqslant 0.333$, whereas the first neighbor distance is $0.779 \leqslant \delta \leqslant 1.139$. The plot of E/N vs. ρ for fluid[10] and solid configuration is displayed in FIGURE 2, where we include the results of the early computation with only $l = 0, 1, 2$. It is concluded that at $\rho = 1.6 \times 10^{15}$ g/cc a neutron gas solidifies into an antiferromagnetic *F.C.C.* structure.

A remark about higher-order terms is appropriate. In systems that are translationally invariant the unperturbed wave function is usually taken to be a plane wave; the general Brueckner theory is a low-density expansion, and it is not obvious that such a method should work, for example, for solid hydrogen or solid helium. Solid hydrogen has recently been studied by Ostgaard,[11] and equation 1 was found to work surprisingly well. According to Ostgaard, this is partly due to the fact that instead of a plane wave one employs gaussian wave function, which already incorporates several correlations.

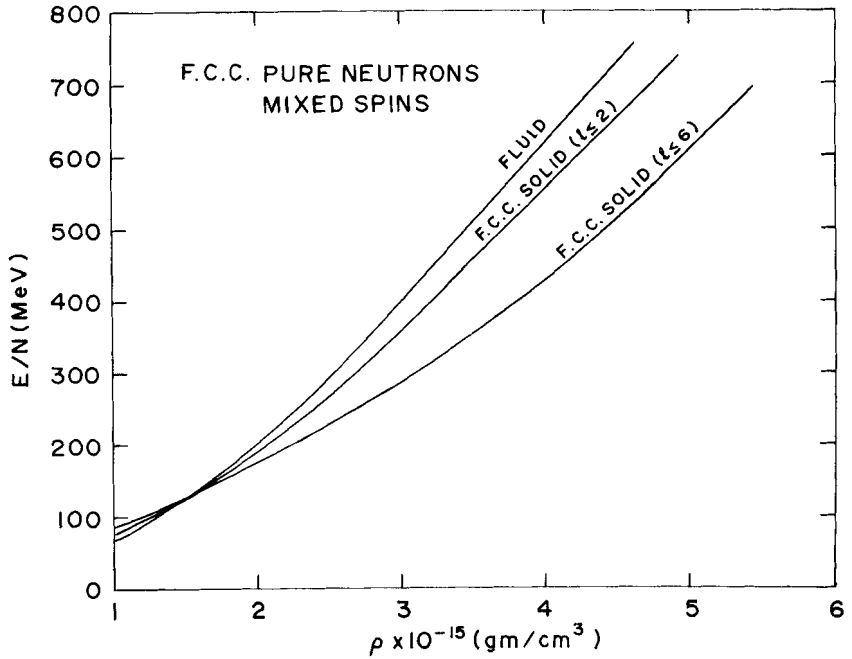

FIGURE 2. Ground-state energy per particle (in MeV) vs the density (in g/cm^3) for neutron FCC lattice and neutron fluid. The fluid curve is taken from Pandharipande's equation of state. Results of earlier lattice computation performed with $l = 2$ are displayed for comparison.

TABLE 1
F.C.C. PURE NEUTRONS, MIXED SPINS

$10^{-15}\rho$	Δ	α^{-1} (*H.F.*)	*E/N*
(g/cm^3)	(fermi)	(fermi)	(MeV)
1.6	1.139	0.333	140
1.83	1.089	0.327	162
2.4	0.995	0.312	210
3.34	0.891	0.274	333
4.0	0.839	0.261	428
4.34	0.817	0.250	495
5.0	0.779	0.238	610

The same can be said about solid ^{3}He. The method outlined in this paper has been applied to ^{3}He, and the results of E/N vs. molar volume are given in FIGURE 3. The inclusion of $l = 6, 7$ was strictly necessary, as shown years ago by Brueckner and Frohberg.[12] In fact, the energy E/N with only $l = 4$ is rather poor with respect to the experimental value. By solving the coupled equations we found $g(r)$ that can be represented by $\theta(r - r_c)$ with $r_c \simeq 2.2$ Å. Even though the t-matrix correlation function has a considerable overshooting and slower healing than the $g(r)$ obtained from variational theories, it does not mean that the three-body effects are more important.[5] Day[5] has in fact demonstrated that E_3 is a function of the two g's;

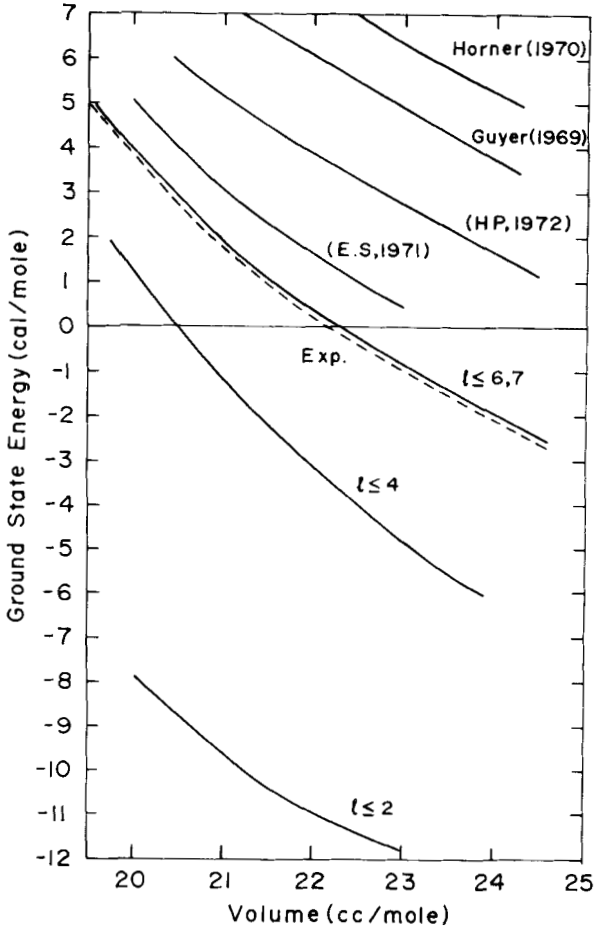

FIGURE 3. Ground-state energy per particle (in cal/mole) vs. molar volume (in cm^3/mole) for solid ^{3}He. Four other theoretical curves are exhibited for comparison.[13-16] The experimental results are from Edwards and Pandorf.[17] For comparison our results are shown for $l = 2$, 4 and 6, 7. The energy values saturate around $l = 6$.

g^{on} and g^{off}, the on-the-energy shell and off-the-energy shell. The latter has almost no overshoot, and g^{off} and g^{on} are equivalent to a g that has almost no overshoot. No detailed study yet exists of g^{on} and g^{off} for ^{3}He or neutron system, and, therefore, no definite conclusion can be drawn. Based on the shape of correlation function obtained with the present method, we shall compute the wound-integral, k, that represents the importance of higher clusters. By definition

$$k = \rho \int |\psi - \phi|^2 d^3r$$

After using $\psi = \phi g$ (See also equation A.11 of Ref. 5), one gets

$$k = \sum_k \frac{N_k}{\delta_k} \frac{\alpha}{\sqrt{2\pi}} \int_0^\infty r dr e^{-(\alpha^2/2)(r-\delta)^2}(1 - g(r))$$

where N_k is the number of neighbors.

For $\alpha^2 = 1.82$, corresponding to a volume of 21 (cm³/mole), k turns out to be 0.135. The value is small enough to make the three-body correlation not overwhelmingly important. Once the energy per particle E/N is known it is a simple matter to compute the energy density and the pressure. We have fitted P, ϵ with a polynomial expression, and the results are

$$\begin{aligned} P_{36} &= 0.5051 - 0.672\,\rho_{15} + 0.295\,\rho_{15}^2 \\ \epsilon_{36} &= 0.648 + 0.326\,\rho_{15} + 0.206\,\rho_{15}^2 \end{aligned} \qquad \rho \geqslant 1.6 \times 10^{15}\ \text{g/cc}$$

where

$$P_{36} = P \cdot 10^{-36}\ \text{dynes/cm}^2, \quad \epsilon_{36} = \epsilon \cdot 10^{-36}\ \text{erg/cm}^3, \quad \rho_{15} = 10^{-15}\,\rho\ \text{g/cc}.$$

For densities lower than 1.6×10^{15} g/cc our P and ϵ join smoothly the equation

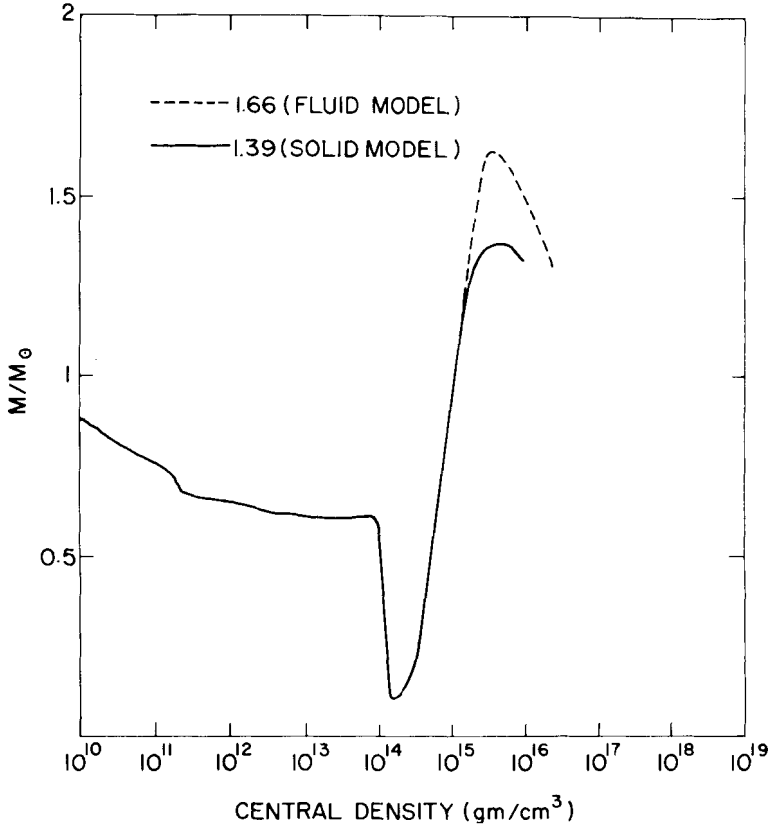

FIGURE 4. Neutron star mass in units of the solar mass vs. the central mass-energy density (in g/cm³). The dashed curve is from Baym and colleagues.[18]

of state of Pandharipande.[10] The general relativistic equations of hydrostatic equilibrium were then integrated, and a plot of $M/M_\odot$ vs. ρ_c (= central mass-energy density) so obtained is displayed in FIGURE 4.

There is an astrophysical piece of evidence to support the idea of a solid core inside heavy neutron stars, and this relates to the fact that the starquake theory of pulsar speedups, which can so plausibly account for the behavior of the Crab pulsar, can explain the observed features of the Vela pulsar only if it is assumed that the Vela possesses a solid core. Pines and colleagues[1] have argued that the solid core has sufficient elastic energy to power the starquakes of the magnitude and frequency observed in the Vela pulsar.

REFERENCES

1. PINES, D., J. SHAHAM & M. A. RUDERMAN. 1972. Nature **237:** 83.
2. BAYM, G., H. A. BETHE & C. PETHICK. 1971. Nucl. Phys. **A175:** 225.
3. ANDERSON, P. W. & R. G. PALMER. 1971. Nature Phys. Sci. **231:** 145.
4. CLARK, J. W. & N. C. CHAO. 1972. Nature Phys. Sci. **236:** 37.
5. BRANDOW, B. H. 1972. Ann. Phys. **74:** 112.
6. NOSANOW, L. H. 1966. Phys. Rev. **146:** 120.
7. GUYER, R. A. & L. I. ZANE. 1969. Phys. Rev. **188:** 445.
8. IWAMOTO, F. & H. NAMAIZAWA. 1971. Progr. Theor. Phys. **45:** 682.
9. BETHE, H. A., B. H. BRANDOW & A. G. PETSCHEK. 1963. Phys. Rev. **129:** 225.
10. PANDHARIPANDE, V. R. 1971. Nucl. Phys. **A174:** 641.
11. OSTGAARD, E. 1972. J. Low. Temp. Phys. **7:** 471.
12. BRUECKNER, K. A. & J. FROHBERG. 1965. Progr. Theor. Phys. Extra Number: 383.
13. EBNER, C. & C. C SUNG. 1971. Phys. Rev. **A4:** 269.
14. GUYER, R. A. 1969. Solid State Comm. **7:** 315.
15. HANSEN, J. P. & E. L. POLLACK. 1972. Phys. Rev. **A5:** 2651.
16. HORNER, H. 1970. Phys. Rev. **A1:** 1722.
17. EDWARDS, D. O. & R. C. PANDORF. 1968. Phys. Rev. **169:** 222.
18. BAYM, G., C. PETHICK & SUTHERLAND. 1971. Ap. J. **170:** 299.